Journal of Biomechanics 46 (2013) 1293–1299

Contents lists available at SciVerse ScienceDirect

Journal of Biomechanics

journal homepage: www.elsevier.com/locate/jbiomech
www.JBiomech.com

Theoretical bounds for the influence of tissue-level ductility on the apparent-level strength of human trabecular bone

Shashank Nawathe [a,*], Frédéric Juillard [a,b], Tony M. Keaveny [a,c,1]

[a] Orthopaedic Biomechanics Laboratory, Department of Mechanical Engineering, University of California, Berkeley, CA, USA
[b] École Polytechnique Fédérale de Lausanne, Lausanne, Switzerland
[c] Department of Bioengineering, University of California, Berkeley, CA, USA

ARTICLE INFO

Article history:
Accepted 11 February 2013

Keywords:
Finite element analysis
Bone quality
Brittle
Ductile
Microarchitecture

ABSTRACT

The role of tissue-level post-yield behavior on the apparent-level strength of trabecular bone is a potentially important aspect of bone quality. To gain insight into this issue, we compared the apparent-level strength of trabecular bone for the hypothetical cases of fully brittle versus fully ductile failure behavior of the trabecular tissue. Twenty human cadaver trabecular bone specimens (5 mm cube; BV/TV=6–36%) were scanned with micro-CT to create 3D finite element models (22-micron element size). For each model, apparent-level strength was computed assuming either fully brittle (fracture with no tissue ductility) or fully ductile (yield with no tissue fracture) tissue-level behaviors. We found that the apparent-level ultimate strength for the brittle behavior was only about half the value of the apparent-level 0.2%-offset yield strength for the ductile behavior, and the ratio of these brittle to ductile strengths was almost constant (mean $\pm$ SD=0.56 $\pm$ 0.02; n=20; R^2=0.99 between the two measures). As a result of this small variation, although the ratio of brittle to ductile strengths was positively correlated with the bone volume fraction (R^2=0.44, p=0.01) and structure model index (SMI, R^2=0.58, $p<0.01$), these effects were small. Mechanistically, the fully ductile behavior resulted in a much higher apparent-level strength because in this case about 16-fold more tissue was required to fail than for the fully brittle behavior; also, there was more tensile- than compressive-mode of failure at the tissue level for the fully brittle behavior. We conclude that, in theory, the apparent-level strength behavior of human trabecular bone can vary appreciably depending on whether the tissue fails in a fully ductile versus fully brittle manner, and this effect is largely constant despite appreciable variations in bone volume fraction and microarchitecture.

1. Introduction

One fundamental issue in bone biomechanics is the influence of tissue-level ductility on the apparent-level strength behavior of trabecular bone. Tissue-level ductility is most easily characterized by the magnitude of the post-yield strain to fracture. While this post-yield strain decreases with aging for cortical tissue (Burstein et al., 1976; Courtney et al., 1996; McCalden et al., 1993; Reilly and Burstein, 1975) and is thought to influence whole-bone fragility (Seeman and Delmas, 2006), many details for trabecular bone remain unclear. In the only study of its type we are aware of, Hernandez et al., (2005) tested 231 individual trabeculae from 32 cadavers to failure in tension, and found relatively large values of ultimate strain (mean $\pm$ SD=8.8% $\pm$ 3.7%). Compared to average ultimate strains for human cortical tissue on the order of about 2% (McCalden et al., 1993), this limited literature suggests that trabecular tissue may be much more ductile than cortical tissue. However, it is difficult to interpret the relevance of such findings without understanding the influence of tissue-level ductility on the apparent-level strength of trabecular bone. This multi-scale issue, which relates ductility at one scale to strength at a higher scale, has been well investigated for composites (Llorca and Gonzalez, 1998; Mortensen and Llorca, 2010) and cellular solid materials (Gibson and Ashby, 1997; Maiti et al., 1984), but less so for trabecular bone. Verhulp (Verhulp et al., 2008b) used micro-CT-based finite element analysis to study the micro-mechanics of bovine trabecular bone and found no appreciable effect of variations in the assumed shape of the post-yield behavior of the tissue on the apparent-level strength. However, they did not address the

* Correspondence to: 2166 Etcheverry Hall, University of California, Berkeley, CA 94720-1740, USA. Tel.: +1 510 642 3787; fax: +1 510 642 6163.
E-mail addresses: shashank@berkeley.edu, nawathe.shashank@gmail.com (S. Nawathe), tmk@me.berkeley.edu (T.M. Keaveny).
[1] **Please address all reprint requests to:** 6175 Etcheverry Hall, University of California, Berkeley, CA 94720-1740, USA. Tel: +1 510 642-8017, fax +1 510 642-6163.

0021-9290/$ - see front matter © 2013 Elsevier Ltd. All rights reserved.
http://dx.doi.org/10.1016/j.jbiomech.2013.02.011

degree of ductility, imposing no limit on the magnitude of the tissue-level strains. Thus, we investigated how the apparent-level trabecular bone strength and the underlying failure mechanisms are altered when the tissue-level failure behavior is changed from fully ductile to fully brittle—the two extremes of possible tissue-level ductility; we also assessed how these effects depend on typical population variations in bone volume fraction and micro-architecture. In this way, we provided theoretical bounds for the influence of tissue-level ductility on the apparent-level strength of human trabecular bone.

2. Materials and Methods

2.1. Specimen preparation and imaging:

We analyzed 20 specimens of human trabecular bone, taken from four anatomic sites, 16 cadavers, both sexes, and spanning a wide range of age and bone volume fraction (Table 1). The specimens were originally machined as 8 mm-diameter cylindrical cores along their principal trabecular orientation, and were scanned at a spatial resolution of 10–22 μm using micro-CT ($n=15$; Scanco Medical AG, Switzerland) or serial milling ($n=5$) (Beck et al., 1997). For this analysis, we virtually extracted out a 5 mm cube from the central portion of each image and resampled all images to a 22-micron voxel size. Measures of bone volume fraction (BV/TV) and standard microarchitecture parameters (Hildebrand et al., 1999; Laib et al., 2001) were obtained from these specimens, the microarchitecture data available only for the 15 specimens scanned with micro-CT. These 15 specimens displayed substantial heterogeneity in the bone volume fraction and microarchitecture (Mean ± SD: BV/TV = 0.16 ± 0.06, SMI = 1.00 ± 0.73, Conn.Den. = 5.78 ± 2.86, Tb.N = 1.39 ± 0.29, Tb.Sp = 0.70 ± 0.14, Tb.Th = 0.17 ± 0.03, Tb.(1/N).SD = 0.26 ± 0.05, Tb.Sp.SD = 0.24 ± 0.06, Tb.Th.SD = 0.06 ± 0.01, and DA = 1.88 ± 0.35).

2.2. Finite element Modeling:

Voxel-based finite element models were generated for each specimen by converting each image voxel in the 5 mm cube to an 8-noded brick element (22 μm element size). This element size fulfilled the convergence requirements (Guldberg et al., 1998; Niebur et al., 1999). In each model, all finite elements were assigned the same hard tissue material properties, having an isotropic elastic modulus of 18.0 GPa (Bayraktar et al., 2004), a Poisson's ratio of 0.3, and failure properties as described below. Displacement roller-type boundary conditions were applied to impose unconstrained uniaxial compression loading.

Table 1
Specimen details for the final cohort.

Anatomic site	No. of specimens[a] (male/female)	Age (years)	Bone volume fraction (mean ± SD)
Femoral Neck	7 (4/3)	69 ± 9	0.25 ± 0.05
Greater Trochanter	3(3/0)	66 ± 10	0.12 ± 0.03
Proximal Tibia	4(4/0)	65 ± 9	0.14 ± 0.04
Vertebral Body	6(4/2)	66 ± 8	0.09 ± 0.03
Pooled	20(15/5)	67 ± 9	0.16 ± 0.06

[a] Number of trabecular bone cube specimens; altogether these specimens were taken from a total of 16 different cadavers.

For each model, two separate non-linear finite element analyses were performed to simulate fully ductile and fully brittle tissue-level behaviors (Fig. 1). For both types of analyses, kinematic large-deformation geometric non-linearity was included in the constitutive model (Bevill et al., 2006; Stolken and Kinney, 2003). All analyses were performed using a highly scalable, implicit parallel finite element framework, Olympus (Adams et al., 2004) on a Sun Constellation Linux Cluster (Ranger; TACC, TX, USA). On average, each fully ductile analysis required about 100 CPU hours and each fully brittle analysis required about 450 CPU hours.

For the fully ductile case, as described in detail elsewhere (Bevill et al., 2006), we assumed tissue-level failure by yielding, using a rate-independent elasto-plasticity type model (Papadopoulos and Lu, 1998). Such yielding comprised a modified von-Mises criterion with tension-compression strength asymmetry (Bayraktar et al., 2004; Niebur et al., 2000), which was achieved by introducing pseudo-kinematic hardening to shift the yield envelope. The tissue-level yield strains of 0.33% in tension and −0.81% in compression were chosen (Bevill et al., 2006). The apparent-level yield strength was obtained from the computed apparent-level stress–strain curves using a 0.2%-offset criterion (Fig. 2). Such measures of apparent-level yield strength have been well validated previously in experiments (Bevill et al., 2006; Sanyal et al., 2012) and are about 83% of, and highly correlated ($R^2=0.96$) with, ultimate strength (Crawford et al., 2003).

For the fully brittle case, element yielding was not allowed and instead we used a quasi-nonlinear approach to simulate brittle fracture of any elements that exceeded the assumed tissue-level yield strengths in either tension or compression. In particular, an elastic analysis was performed to a specified apparent-level strain; stresses were computed at each element centroid, as was the overall apparent-level stress for the whole specimen. Once either the maximum or minimum principal stress at any element centroid exceeded the assumed respective tissue-level tensile or compressive yield strength, that element was assumed to fail in a brittle manner and we reduced its elastic modulus 100-fold for subsequent analyses. Using these reduced properties in all such failed elements, a new elastic analysis was then performed for the whole specimen to an incrementally higher apparent-level strain. This whole process was repeated until we generated an overall apparent-level stress–strain curve that displayed an ultimate point. Typically for each of these fully brittle analyses, 20 increments of apparent-level strain were applied, and thus 20 geometrically non-linear but otherwise elastic analyses were performed. The apparent-level ultimate strength was defined as the maximum stress on the computed apparent-level stress–strain curve. An apparent-level 0.2%-offset yield strength was not used for these brittle analyses since the corresponding yield strain was greater than the ultimate strain (Fig. 2).

To aid in interpretation of the results, we also performed an ancillary parametric sub-study on three trabecular bone specimens wherein the tissue-level compressive strength was altered while keeping the tissue-level tensile strength constant.

2.3. Cellular solid analysis

To provide additional insight, we also used cellular solid theory (Gibson and Ashby, 1997) to derive an analytical expression for the ratio of brittle to ductile strengths. As described elsewhere (Cowin, 2001; Gibson and Ashby, 1997; Keaveny, 2001), we assumed a 2D honeycomb-like structure with a hexagonal

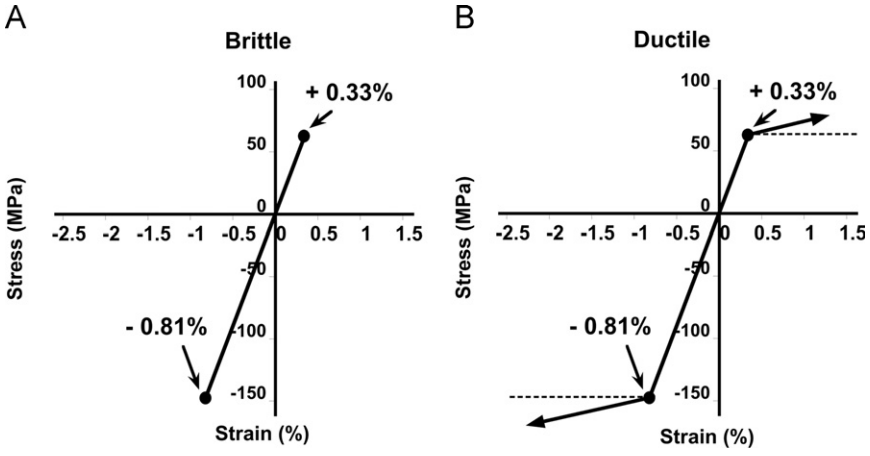

Fig. 1. Material models depicting the stress–strain response at the tissue-level for: (A) fully brittle, and (B) fully ductile bone tissue.